Supplemental material : Size effect on the structural and magnetic phase transformations of iron nanoparticles

Alexis Front,[1,2,3] Georg Daniel Förster,[4] Chu-Chun Fu,[5] Cyrille Barreteau,[6] and Hakim Amara[1,7]

[1] *Laboratoire d'Etude des Microstructures, ONERA-CNRS, UMR104, Université Paris-Saclay, BP 72, Châtillon Cedex, 92322, France*
[2] *Department of Chemistry and Materials Science, Aalto University, 02150 Espoo, Finland*
[3] *Department of Applied physics, Aalto University, FI-00076 Aalto, Espoo, Finland*
[4] *Interfaces, Confinement,Matériaux et Nanostructures (ICMN), CNRS, Université d'Orléans, 45071, Orléans, France*
[5] *Université Paris-Saclay, CEA, Service de recherche en Corrosion et Comportement des Matériaux, SRMP, F-91191 Gif-sur-Yvette, France*
[6] *SPEC, CEA, CNRS, Université Paris-Saclay, CEA Saclay, F-91191 Gif-sur-Yvette, France*
[7] *Université Paris Cité, Laboratoire Matériaux et Phénomènes Quantiques (MPQ), CNRS-UMR7162, 75013 Paris, France*

(Dated: August 29, 2024)

Sec. I. Magnetic tight-binding model

In the following, a brief description of the key features of our interatomic potential for treating magnetic transition metals and its transferability is provided. For the technical and theoretical aspects, a detailed account of the TB model is given in the following references[1,2] while the fitting of the parameters to reproduce the energetic properties of Fe is presented.

In our study, the interaction between iron atoms is treated within the semi-empirical tight-binding model[3,4] where only d bands are taken into account. As in non-magnetic systems, the total energy of an atom i is split in two parts, a band structure term that describes the formation of an energy band when atoms are assembled and a repulsive term which empirically reflects the ionic and electronic repulsions. We employ the recursion method to calculate the local density of electronic states $n_i(E)$ at all sites[1,5]. Exact calculations are made of only the first four continued fraction coefficients, (a_1, b_1, a_2, b_2) corresponding to the first four moments of the local density of states. In addition, the magnetic contribution is introduced via the Stoner model[4,6] by considering the physical presence of local exchange fields in the band energy term giving rise to two spin populations within the collinear approximation. Besides, the fourth moment approximation (FMA) is a good compromise for describing the structural properties of transition metals[1,2] while having a minimal description of the density of states necessary to take into account local magnetic on-site levels and thus define two spin populations. Interestingly, the FMA model is highly effective to enable a linear scaling of CPU working time as a function of system size. This magnetic TB model relies on local (atomic) energy calculations is coupled with Monte Carlo (MC) simulations in order to relax the structures where each trial corresponds to randomly choosing an atom and its displacement as well as its local magnetic moment. By performing this procedure several times, it becomes possible to determine the equilibrium properties of iron nanoparticles of various sizes in terms of both position and magnetic state.

Sec. II. Iron tight-binding model

In case of transition metals, the electronic structure is defined by a narrow d band hybridizing with a wider sp-band corresponding to nearly free electrons. Given that the cohesion properties of Fe are mainly driven by $d-d$ bonding, it is only necessary to include d orbitals in the spin-polarised TB framework[7]. In our d band model, the Slater-Koster parameters characterizing the hopping integrals ($dd\sigma$, $dd\pi$ and $dd\delta$) are chosen according to the ratio -2:1:0 and to decrease exponentially with the following distance dependence r between atoms:

$$dd\lambda(r) = dd\lambda_0 \exp\left[-q\left(\frac{r}{r_0}-1\right)\right] \quad , \tag{1}$$

where $\lambda = \sigma, \pi, \delta$ and q a parameter to be fitted. Regarding the repulsive term, a Born-Mayer expression has been adopted involving two additional parameters (A and p):

$$E^i_{\text{rep}} = A\sum_{j\neq i} \exp\left[-p\left(\frac{r_{ij}}{r_0}-1\right)\right] \tag{2}$$

To capture all magnetic effects, the Stoner exchange integral I is the only additional parameter to be included in our TB model. This results in an energy contribution of $-\frac{I}{4}m_i^2$[8] where m_i is the spin moment in μ_B units. Indeed, $m_i = N_i\uparrow - N_i\downarrow$ with $N_i\uparrow$ and $N_i\downarrow$, respectively the number of electrons in majority and minority spin bands of an atom i. To get an efficient interatomic potential, the parameters ($dd\sigma$, q, A, p and I) and the number of electrons N_d have to be adjusted to reproduce several bulk physical properties of Fe.

All the difficulty is to define the relevant quantities specific to Fe, both from a structural and magnetic point of view, for the development of an interatomic potential with a high degree of transferability to study phase transformation of magnetic Fe NPs. In the present work, the TB parameters have been fitted on experimental

$dd\sigma$	q	r_0	A	p	I	N_d
1.08	3.29	2.42	0.166	10.5	1.15	7.59

TABLE S1. Fe parameters for the magnetic TB-FMA model, obtained by fitting to DFT reference data. $dd\sigma$, A and I are in eV. r_0 is in Å.

data and density functional theory (DFT) calculations using the Vienna *ab initio* Simulation Package (VASP) code[9] to reproduce the lattice parameter, the cohesive energy, the elastic moduli (bulk modulus and the two shear moduli) and the magnetism state of α and β bulk Fe phases at 0 K. The resulting parameter values are given in Table S1.

Sec. III. Validity and transferability of the tight-binding model

The TB parameters have been fitted on experimental values for the FCC and BCC structures namely the lattice parameter, the cohesive energy and the elastic moduli (bulk modulus and the two shear moduli) as well as their magnetic properties. All results are presented in Table S2.

As already discussed[10,11], ferromagnetism clearly plays a major role in determining the stability of bulk Fe structures. It is interesting to note that our model successfully reproduces the main trends of this specific physics. Indeed, when magnetism is not taken into account, the β structure is the most stable. Such behavior of non-magnetic calculations has been highlighted in previous calculations[11,12]. Nevertheless, magnetic calculations correct this and reproduce the experimentally stable phase, i.e. the ground-state FM α-Fe structure which is also successfully predicted by the TB potential. Moreover, regarding the dependencies of magnetic moments as function of the lattice parameters, our TB results are in agreement with the DFT calculations in particular the increase in magnetic moment as the structures are expanded. To highlight how the ground state is driven by the magnetism, the analysis of elastic constants (C_{ij}) is very relevant. In case of the cubic phase, three independent elastic constants (C_{11}, C_{12} and C_{44}) have to be considered, or even their combination giving rise to the tetragonal shear modulus, $C' = (C_{11} - C_{12})/2$, and the bulk modulus, $B = (C_{11} + 2C_{12})/3$. Note that a negative value means that the system is mechanically unstable. As seen in Table S2, they are calculated for non-magnetic and ferromagnetic BCC and FCC iron from our TB model, and compared with experimental as well as DFT results. It is immediately striking that the general trends are perfectly reproduced by the TB model. More specifically, it predicts correctly negative values of C' for the NM BCC structure and a positive one for the ferromagnetic BCC confirming its stability respect to the tetragonal distortion. This particular behaviour is perfectly illustrated in the analysis of the energy along the Bain transformation path connecting the BCC ($c/a = 1$) and FCC ($c/a = \sqrt{2}$) structures and presented in Figure S1. Although the energy

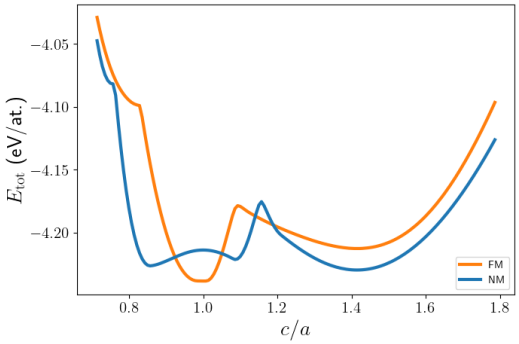

FIG. S1. Bain path between the BCC and FCC phases in case of NM and FM calculations.

difference between the ferromagnetic and non-magnetic configurations is underestimated by the TB model, the overall trend of the energy profile is in good agreement with previous DFT calculations[11]. Consequently, it can be seen that the TB model is not only well suited to discriminate between the different magnetic phases of Fe, but also has the ability to predict quite subtle characteristics, such as the link between the magnetism and the structural stability of the BCC phase under tetragonal deformation. To go further in the validation and transferability of the interatomic potential for studying thermodynamic properties, it is fundamental to assess its reliability at finite temperature. In this context, the Curie temperature is investigated and results are presented in Figure S2a. Our TB model predicts a T_C^∞ around 500 K which is much lower than the experimental value of 1043 K. Improving the accuracy of the calculated Curie temperature can be done by tuning the Stoner parameter as explained in Reference[2]. However, it turns out that properties at 0K are more difficult to reproduce in this case. Nevertheless, this deviation in the calculation of the Curie temperature does not prevent us from describing qualitatively structural and magnetic properties of Fe NPs as we will see in the following since all the results will be discussed in relation to a value of T_C^∞ which is simply a reference in our study. Again with the aim of studying the behaviour of our TB model at finite temperature, Figure S2b displays the temperature dependencies of the thermal expansion coefficient in case of NM and FM calculations. A linear variation is then observed for the NM case, in contrast to the FM calculations where a contraction of the lattice parameter is reported in agreement with experiments[13]. Our TB model is therefore capable of capturing such a feature, unlike many of the interatomic potentials presented in the literature.

		NM DFT	NM TB-FMA	FM DFT	FM TB-FMA
BCC	a (Å)	2.76	2.73	2.83	2.86
	E_{coh} (eV/at.)	-3.81	-4.21	-4.28	-4.24
	C_{11}, C_{12}, C_{44} (GPa)	89, 351, 186	219, 272, 87	278, 144, 97	157, 143, 95
FCC	a (Å)	3.45	3.43	3.48	3.58
	E_{coh} (eV/at.)	-4.12	-4.23	-4.13	-4.21
	C_{11}, C_{12}, C_{44} (GPa)	430, 223, 244	306, 233, 81	318, 127, 178	179, 132, 58

TABLE S2. DFT and TB calculations of physical properties for non magnetic and magnetic bcc and fcc systems at 0 K.

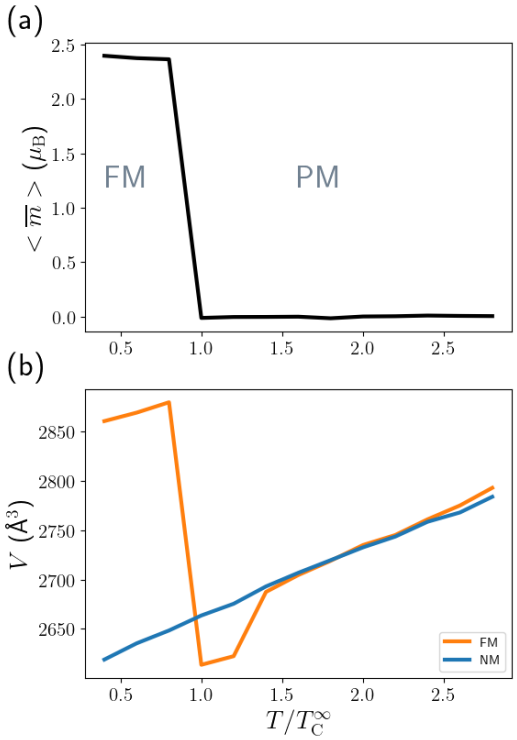

FIG. S2. (a) Total magnetic moment average of a bulk Fe as a function of temperature. (b) Average linear volume expansion coefficient for Fe as a function of temperature (FM and NM states).

[1] H. Amara, J.-M. Roussel, C. Bichara, J.-P. Gaspard, and F. Ducastelle, "Tight-binding potential for atomistic simulations of carbon interacting with transition metals: Application to the ni-c system," Phys. Rev. B **79**, 014109 (2009).

[2] A. Front, G. D. Förster, V.-T. Tran, C.-C. Fu, C. Barreteau, F. Ducastelle, and H. Amara, "Simulation of thermodynamic properties of magnetic transition metals from an efficient tight-binding model: The case of cobalt and beyond," Phys. Rev. B **105**, 144101 (2022).

[3] F. Ducastelle, Order and Phase Stability in Alloys (North Holland, 1991).

[4] D.G. Pettifor, Bonding and Structure in Molecules and Solids (Oxford University Press, 1995).

[5] J. H. Los, C. Bichara, and R. J. M. Pellenq, "Tight binding within the fourth moment approximation: Efficient implementation and application to liquid ni droplet diffusion on graphene," Phys. Rev. B **84**, 085455 (2011).

[6] E. Stoner, "Collective electron ferromagnetism ii. energy and specific heat," Proc. Roy. Soc. A **169**, 339 (1939).

[7] Ducastelle, F., "Modules élastiques des métaux de transition," J. Phys. France **31**, 1055–1062 (1970).

[8] Michael E Ford, Ralf Drautz, Thomas Hammerschmidt, and D G Pettifor, "Convergence of an analytic bond-order potential for collinear magnetism in fe," Modelling and Simulation in Materials Science and Engineering **22**,

034005 (2014).
[9] G. Kresse and D. Joubert, "From ultrasoft pseudopotentials to the projector augmented-wave method," Phys. Rev. B **59**, 1758–1775 (1999).
[10] H. C. Herper, E. Hoffmann, and P. Entel, "Ab initio full-potential study of the structural and magnetic phase stability of iron," Phys. Rev.B **60**, 3839–3848 (1999).
[11] M. Mrovec, D. Nguyen-Manh, C. Elsässer, and P. Gumbsch, "Magnetic bond-order potential for iron," Phys. Rev. Lett. **106**, 246402 (2011).
[12] G. Autès, C. Barreteau, D. Spanjaard, and M.-C. Desjonquères, "Magnetism of iron: from the bulk to the monatomic wire," J. Phys.: Condens. Matter **18**, 6785 (2006).
[13] Y.C Liu, F Sommer, and E.J Mittemeijer, "Calibration of the differential dilatometric measurement signal upon heating and cooling; thermal expansion of pure iron," Thermochimica Acta **413**, 215–225 (2004).